JOURNAL OF COMPUTATIONAL PHYSICS 2, 363–380 (1968)

Finite-Difference Approximation of the Exterior Problem for Poisson's Equation

C. NELSON DORNY

The Moore School of Electrical Engineering, University of Pennsylvania, Philadelphia, Pennsylvania 19104

ABSTRACT

The three-dimensional exterior problem (where the potential distribution is outside of the boundary configuration) is converted to an equivalent interior problem, while leaving the region of interest unchanged. The important axially symmetric problem is treated as a special case. Finite-difference approximations appropriate for computer solution of the modified exterior problem are proposed for both the two-dimensional (x–y coordinate) and the axially symmetric (r–z coordinate) cases. The accuracy of these finite-difference approximations is evaluated by numerical solution of exterior problems with known analytical solutions.

1. INTRODUCTION

In many practical engineering design problems where a solution to Poisson's equation is desired, the potential distribution of interest is outside of the boundary configuration, and extends to infinity. A simple example of such a problem is the determination of the magnetic field about an isolated bar magnet. Before a finite-difference solution to such a problem can be obtained, the exterior problem must be converted to a problem with a finite domain, in order to avoid an infinite number of grid points.

Several authors have developed schemes for approximating an exterior problem by a finite problem. Matheson and Luenberger [1] enclose the region of interest by an equipotential box which is large enough to have little effect on the potential in that region. Ryan [2], using a resistance analog to solve the difference equations, obtains a resistor termination network for use at the boundary of the region of interest. Boothroyd, Cherry, and Makar [3] use conformal mapping to convert the two-dimensional exterior problem for Laplace's equation into an exactly equivalent interior problem, while leaving the region of interest unchanged.

This paper extends the results of Boothroyd, Cherry, and Makar to the solution of Poisson's equation in three dimensions and to the very practical axially-sym-

metric case (r–z coordinates). In addition, finite-difference approximations appropriate for computer solution of the modified exterior problem are proposed for both x–y and r–z coordinates. The accuracy of these approximations is evaluated by numerical solution of exterior problems with known analytical solutions.

2. The Exterior–Interior Transformation in Two Dimensions

Although rectangular coordinates seem the natural choice for representation of two-dimensional problems, polar coordinates will be more appropriate for this derivation. Let $u(r, \theta)$ denote the potential distribution of the exterior problem; that is, $u(r, \theta)$ satisfies Poisson's equation everywhere except where boundary conditions are specified. Assume that $u(r, \theta)$ is bounded near infinity, and that the region of interest is totally contained within the disk $r \leqslant a$ [see Fig. 1(a)]. Define the transformed potential $v(r, \theta)$ by inversion in the circle of radius a,

$$v(r, \theta) \equiv u(a^2/r, \theta). \tag{1}$$

The inside of the circle is mapped outside, and vice versa; the origin for $v(r, \theta)$ corresponds to the point infinity for $u(r, \theta)$[see Fig. 1(b)].

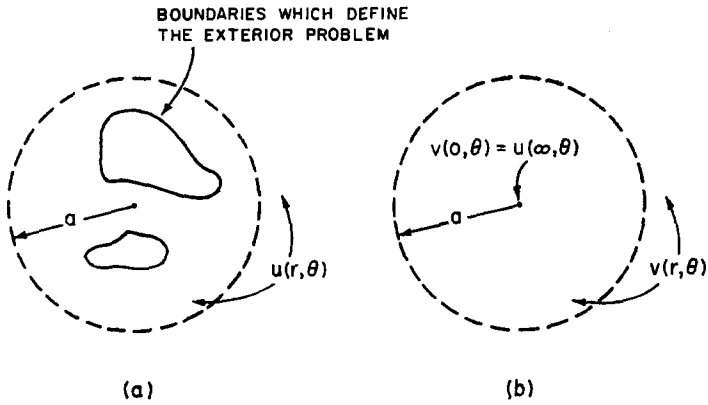

Fig. 1. Inversion in the circle.

We will show that $v(r, \theta)$ can also satisfy Poisson's equation. Defining $\beta = a^2/r$, and letting subscripts denote partial derivatives,

$$\nabla^2 v(r, \theta) \equiv v_{rr}(r, \theta) + \frac{1}{r} v_r(r, \theta) + \frac{1}{r^2} v_{\theta\theta}(r, \theta)$$

$$= \frac{\partial^2}{\partial r^2} u\left(\frac{a^2}{r}, \theta\right) + \frac{1}{r} \frac{\partial}{\partial r} u\left(\frac{a^2}{r}, \theta\right) + \frac{1}{r^2} \frac{\partial^2}{\partial \theta^2} u\left(\frac{a^2}{r}, \theta\right)$$

$$= \left(-\frac{a^2}{r^2}\right)^2 u_{\beta\beta}(\beta, \theta) + \frac{2a^2}{r^3} u_{\beta}(\beta, \theta) - \frac{a^2}{r^3} u_{\beta}(\beta, \theta) + \frac{1}{r^2} u_{\theta\theta}(\beta, \theta)$$

$$= \frac{a^4}{r^4}\left[u_{\beta\beta}(\beta, \theta) + \frac{1}{\beta} u_{\beta}(\beta, \theta) + \frac{1}{\beta^2} u_{\theta\theta}(\beta, \theta)\right]$$

$$= \frac{a^4}{r^4} \nabla^2 u(\beta, \theta).$$

By definition,

$$\nabla^2 u(\beta, \theta) = -\frac{1}{\epsilon} \sigma(\beta, \theta), \tag{2}$$

where $\sigma(\beta, \theta)$ is the two-dimensional charge density[1] and ϵ is a constant of the material. Therefore,

$$\nabla^2 v(r, \theta) = -\frac{1}{\epsilon} \frac{a^4}{r^4} \sigma\left(\frac{a^2}{r}, \theta\right). \tag{3}$$

When the position of the charge distribution is inverted in the circle, the charge density must be multiplied by a^4/r^4, where r is the new radius. This requirement guarantees that the total charge in a region before transformation equals the charge in the inversion of that region after transformation. The weighting of the charge distribution is all that is required in order that $v(r, \theta)$ satisfy Poisson's equation.

There is one apparent difficulty. For $r = 0$, the right side of Eq. (3) need not exist. It has been shown that an isolated singularity of a bounded harmonic function is removable. See Kellogg [4]. If the charge density of the original problem is zero in some neighborhood of infinity, then $v(r, \theta)$ satisfies Laplace's equation in a neighborhood of $r = 0$, and the singularity is removable. We impose no practical restriction by requiring that the charge density within some neighborhood of infinity be zero. Since the potential distribution near infinity is of no interest, even a point charge at infinity can be approximated arbitrarily closely by a charge distribution which satisfies this assumption.

Notice that the information contained in $u(r, \theta)$ for $r \geqslant a$ is equivalent to that contained in $v(r, \theta)$ for $r \leqslant a$. The original problem is completely characterized by the potential distributions $v(r, \theta)$ and $u(r, \theta)$ for $r \leqslant a$; the latter is the unmodified potential in the region of interest. These facts motivate us to construct a new problem, defined on a finite domain, from the functions $u(r, \theta)$ and $v(r, \theta)$ in the interiors of the disk-shaped regions. Hereinafter, $u(r, \theta)$ and $v(r, \theta)$ for $r > a$ will be of no interest.

[1] Although the notation and terminology are those associated with electrostatics, the results apply to other steady-state fields as well.

It is easily verified from Eq. (1) that, at $r = a$,

$$\left.\begin{aligned} v(a, \theta) &= u(a, \theta), \\ \frac{\partial}{\partial r} v(a, \theta) &= -\frac{\partial}{\partial r} u(a, \theta). \end{aligned}\right\} \tag{4}$$

These identities define complementary boundary conditions at the edges of the two disks. The new problem, with finite domain, is obtained as follows. The disk-shaped region in which $v(r, \theta)$ is defined is placed behind the disk-shaped region in which $u(r, \theta)$ is defined. The two disks are connected along the circle $r = a$ (see Fig. 2). From Eqs. (4) we see that both the potential and its gradient (the flux density) are continuous across the circular interface; Poisson's equation is satisfied on the complete "double disk" by the potential consisting of $u(r, \theta)$ on the front disk and $v(r, \theta)$ on the rear disk. In essence, the infinite region of the original problem—that part outside $r = a$—has been mapped into a finite region—the "back" of the disk-shaped region of interest—without changing the conditions at the interface $r = a$.

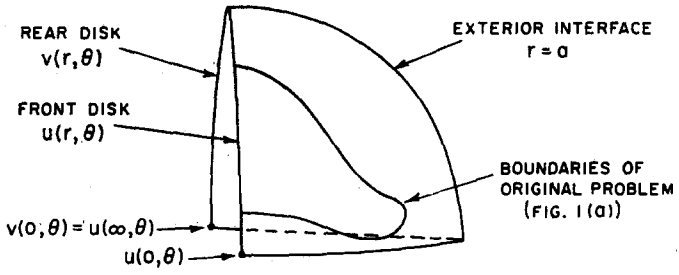

FIG. 2. A portion of the two disks showing their interface at $r = a$.

The fact is well known that the voltage and current in a thin uniform sheet of resistive material correspond to potential and flux. This analogy is often exploited in the experimental determination of potential distributions. The mapping described above may be interpreted as follows. Suppose that both sides (and the edges) of a thin nonconducting disk are coated with a uniform resistive material, and certain boundary conditions are fixed on one side of the disk. Then, the potential distribution on that side of the disk is the same as it would be if that side of the disk were part of an infinite resistive sheet. Thus, an exterior problem for Poisson's equation can be represented by an equivalent "double-disk" interior problem without changing the potential distribution in the region of interest [3].

3. The Exterior–Interior Transformation in Three Dimensions

For the derivation of an exterior–interior transformation which is applicable in three dimensions, it is convenient to use spherical coordinates. The notation is indicated in Figure 3.

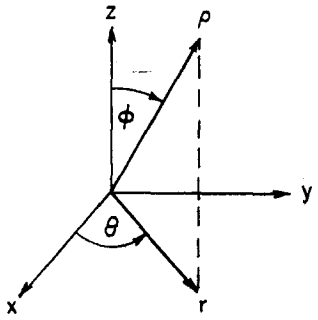

FIG. 3. Relationship between common coordinate systems.

Let $u(\rho, \theta, \phi)$ be the potential distribution, and assume that the region of interest is contained within the sphere $\rho \leqslant a$. Define $v(\rho, \theta, \phi)$ by a modified inversion in the sphere,[2]

$$v(\rho, \theta, \phi) = \frac{a}{\rho} u\left(\frac{a^2}{\rho}, \theta, \phi\right). \tag{5}$$

By repeating the steps used to obtain Eq. (3), we find that

$$\begin{aligned} \nabla^2 v(\rho, \theta, \phi) &\equiv v_{\rho\rho} + \frac{2}{\rho} v_\rho + \frac{\cot \phi}{\rho^2} v_\phi + \frac{1}{\rho^2} v_{\phi\phi} + \frac{1}{\rho^2 \sin^2 \phi} v_{\theta\theta} \\ &= -\frac{1}{\epsilon}\left(\frac{a^5}{\rho^5}\right) \sigma\left(\frac{a^2}{\rho}, \theta, \phi\right). \end{aligned} \tag{6}$$

Thus, v satisfies Poisson's equation if the charge density is multiplied by a^5/ρ^5 (where ρ is the new radius) when its position is transformed in the sphere.

Note that the potential distributions $u(\rho, \theta, \phi)$ and $v(\rho, \theta, \phi)$ defined on $\rho \leqslant a$ completely characterize the original problem. After comparison with the two-dimensional case, one is motivated to attempt construction of a new problem by joining (at $\rho = a$) the interiors of the two spheres where the potentials u and v are defined—in an abstract sense, placing the spheres back to back—and ignoring the potentials for $\rho > a$.

[2] This inversion, called the Kelvin transformation, is the only three-dimensional transformation which preserves Laplace's equation. See Kellogg [4].

From Eq. (5) it is easily verified that at $\rho = a$,

$$v(a, \theta, \phi) = u(a, \theta, \phi) \tag{7}$$

and

$$\frac{\partial}{\partial \rho} v(a, \theta, \phi) = -\frac{\partial}{\partial \rho} u(a, \theta, \phi) - \frac{1}{a} u(a, \theta, \phi). \tag{8}$$

It is clear from Eq. (8) that the boundary conditions at the edges of the two spheres do not complement each other as they did in the two-dimensional case. Interpreted from a physical standpoint,[3] Eq. (8) requires that a surface charge density $-(\epsilon/a)\, u(a, \theta, \phi)$, which is proportional to the potential, be added at the interface in order that the two spheres be joined at $\rho = a$. That is, such a charge density distributed on the sphere $\rho = a$ provides a reason for the discontinuity in the derivative of the potential normal to the sphere. With the addition of such a charge distribution, a three-dimensional exterior problem can be converted to an equivalent "double sphere" interior problem for Poisson's equation while leaving the region of interest unchanged.

4. Axial Symmetry

Physical problems are typically three-dimensional and often cannot be adequately represented in two-dimensional rectangular coordinates. Yet, practical difficulties make finite-difference solution of three-dimensional problems unlikely at the present time. Fortunately, a large percentage of these problems are nearly axially symmetric and can be represented in two-dimensional r–z coordinates (see Fig. 3). The three-dimensional exterior-interior transformation is valuable primarily because it applies in the r–z coordinate case.

Axial symmetry implies that the potential does not vary with θ, but only with r and z (or the equivalent, ρ and ϕ). The transformation of Eq. (5) reduces to a transformation from the outside to the inside of a half disk (see Fig. 4). The explicit mention of θ in Eq. (5) merely emphasizes the three-dimensional nature of the problem. The exterior problem, described in two-dimensional ρ–ϕ coordinates on the half plane, is replaced by a "double half-disk" interior problem. The infinite part of the original problem is mapped onto the back of the half-disk region of interest, analogous to the true two-dimensional case. Poisson's equation is satis-

[3] The component of flux density normal to the sphere is defined as $\epsilon\, \partial u/\partial \rho$ [5].

fied (in ρ–ϕ or r–z coordinates) over each half disk. However, a charge density $-(\epsilon/a)\, u(a, \phi)$ is distributed on the semicircle $\rho = a$ in order to match conditions at this interface.

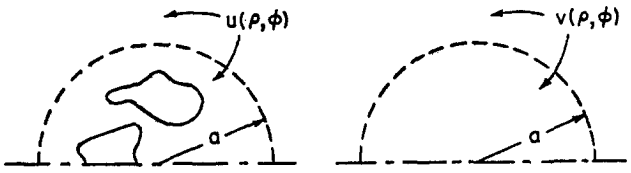

FIG. 4. Inversion with axial symmetry.

5. FINITE-DIFFERENCE REPRESENTATION FOR x–y COORDINATES

The double-disk representation of the two-dimensional exterior problem has a finite domain; therefore, it is suitable for finite-difference approximation. The transformation of the exterior problem to an interior problem has added one more boundary—the exterior interface—to the original boundaries of the problem. In this section a finite-difference approximation to Poisson's equation in the neighborhood of the exterior interface is derived under the assumption of a uniform square grid of spacing h. This approximation is appropriate for a general purpose computer program which uses standard finite-difference approximations in x–y coordinates for the other types of boundary conditions [6]–[8].

The edge of each disk (Fig. 2) is perturbed in order to fit a square grid (see Fig. 5). This perturbation simplifies the estimation of derivatives required by the finite-difference method. In Fig. 6 the perturbed interface is drawn, for clarity, as a piecewise linear curve. At the perturbed interface, both the potential and its normal derivative are continuous.

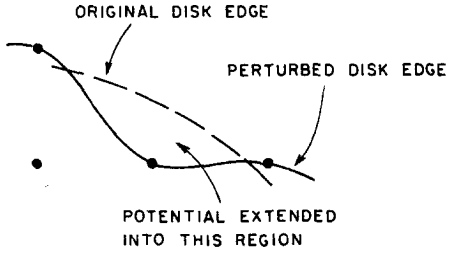

FIG. 5. Intersections of the original circular edge and the perturbed edge of one disk. The front and rear disks are perturbed identically.

In order to simplify the following convergence analysis, assume that the charge density is zero near the edge of each disk. Note that the perturbed edge of each disk occasionally intersects its original circular edge. Assume that the potential distributions of the perturbed double-disk problem (call them U and V) can be extended by analytic continuation across the perturbed edges of each disk far enough to include the regions between intersections of the two curves. See Fig. 5. It is clear that as the grid is refined, the extended potential U at a point on the original edge of the front disk and the extended potential V at the corresponding point on the rear disk both approach the potential at a common point on the perturbed interface. Thus, in the limit, the first condition of Eqs. (4) is satisfied.

Gauss's Flux theorem, which is equivalent to Poisson's equation, states (in three dimensions)

$$-\int_S \epsilon \Phi_n \, dS = Q \tag{9}$$

for each closed surface S, where Φ is the potential, Φ_n is the derivative of Φ in the direction of the outward normal to S, ϵ is a constant of the material, and Q is the total charge enclosed by S (see Reference [4]). Physically, Eq. (9) says that the total flux leaving a region equals the total charge enclosed in that region. In the x–y coordinate case, where Φ does not vary with z, Eq. (9) reduces to

$$-\int_L \epsilon \Phi_n \, dL = Q \tag{10}$$

for each closed curve L; that is, flux does not flow in the z direction.

Letting the path L of Eq. (10) be the boundary of the region between two consecutive intersections of the original and perturbed edges of each disk, and recalling that $Q = 0$ in this region, we find

$$\int_{\text{pert.}} U_n \, dL + \int_{\text{orig.}} U_n \, dL = 0$$

and

$$\int_{\text{pert.}} V_n \, dL + \int_{\text{orig.}} V_n \, dL = 0$$

Along the original circular edges, $U_n \equiv \partial U/\partial r$ and $V_n \equiv \partial V/\partial r$. At the perturbed interface, $U_n = -V_n$. Therefore,

$$\int_{\text{orig.}} \frac{\partial V}{\partial r} \, dL = -\int_{\text{pert.}} V_n \, dL = \int_{\text{pert.}} U_n \, dL = -\int_{\text{orig.}} \frac{\partial U}{\partial r} \, dL. \tag{11}$$

Thus, between intersections the integrated effect of the second condition of (4) is correct. As the grid is refined,

$$\frac{\int_{\text{orig.}} (\partial V/\partial r)\, dL}{\int_{\text{orig.}} dL} \to \frac{\partial V}{\partial r} \quad \text{and} \quad \frac{\int_{\text{orig.}} (\partial U/\partial r)\, dL}{\int_{\text{orig.}} dL} \to \frac{\partial U}{\partial r}$$

at corresponding points on the original circular edges; in the limit, the normal derivative boundary condition of Eqs. (4) is satisfied.

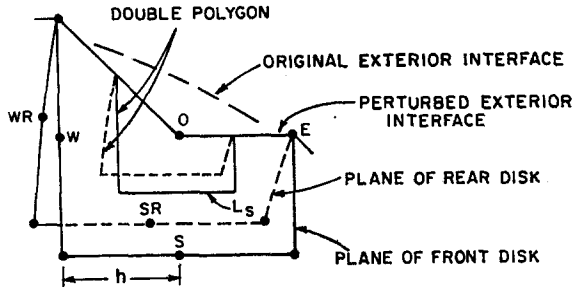

FIG. 6. Typical configuration of grid points at the interface between the two disks.

The front and rear disks of the perturbed exterior problem are represented by identical networks of grid points. Figure 6 shows the manner in which the grid-point approximations to the two disks are joined at the perturbed interface. The point O in that figure represents the "double" polygonal region which extends half way to the neighboring grid points. Let Q_O represent the total charge contained in this region. The grid points which are neighbors to point O are labeled according to the compass, those on the rear disk being distinguished by the extra letter R.

The integration method of deriving the difference equations consists in approximating Eq. (9) [or Eq. (10)] on the region represented by each grid point [6], [8]. Derivation of the finite-difference approximation corresponding to point O of Fig. 6 indicates, by example, how Poisson's equation may be represented in the neighborhood of the perturbed interface of the double disk. Derivatives of the potential normal to the boundary of the double polygon are estimated by potential differences, and are approximately constant over each straight line segment of the polygon. Thus, the flux crossing the south boundary L_S of the polygon on the front disk is approximated by

$$-\int_{L_S} \epsilon \Phi_n\, dL \approx -\epsilon \left(\frac{\Phi_S - \Phi_O}{h}\right) \int_{L_S} dL$$

$$= -\epsilon(\Phi_S - \Phi_O), \tag{12}$$

where Φ_S and Φ_O are potentials at the points S and O, respectively. The total flux leaving the double polygon is estimated by adding together terms similar to Eq. (12) for each segment of the boundary of the polygon. This procedure leads to the following approximation to Eq. (10).[4]

$$-\epsilon(\Phi_S - \Phi_O) - \epsilon(\Phi_{SR} - \Phi_O) - \epsilon(\Phi_W - \Phi_O) - \epsilon(\Phi_{WR} - \Phi_O) - \epsilon(\Phi_E - \Phi_O) = Q_O \tag{13}$$

Note that the configuration of the double polygon represented by the point 0 is determined by the configuration of the perturbed interface. Equation (13) can be rewritten

$$5\Phi_O = \Phi_S + \Phi_{SR} + \Phi_W + \Phi_{WR} + \Phi_E + \frac{Q_O}{\epsilon}, \tag{14}$$

making explicit the manner in which the potential at point O depends upon the potentials at the neighboring points.

6. Two-Dimensional Example

The exterior problem shown in Fig. 7, representing a pair of oppositely charged cylinders, has a known analytical solution [5]. The error which is introduced by the steps described in this paper; viz., the exterior–interior mapping, perturbation of the exterior interface, and finite-difference approximation of the modified exterior problem, is analyzed by actual solution of this example. Because of symmetry in the configuration, the northeast quadrant of the problem is sufficient to define this solution.

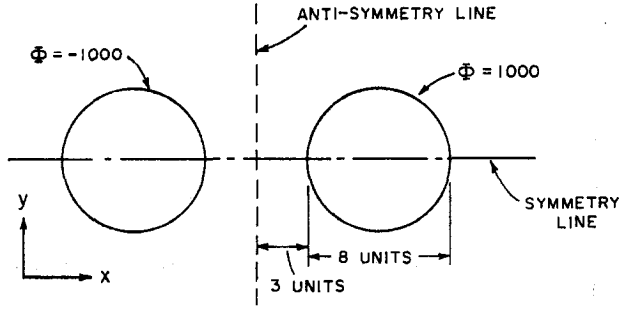

FIG. 7. A pair of oppositely charged circles (cylinders). The potential satisfies $\nabla^2\Phi = 0$.

[4] Dorny [6] shows that approximations of this type lead to a matrix of difference equations which is symmetric, diagonally dominant, and possesses property (A).

Figure 8 shows the perturbed front disk of the modified exterior problem along with the grid-point representation of the exterior interface and the fixed potential circle. (The rest of the grid points are omitted from the figure for clarity.) If the grid points on the rear disk are mapped back onto the infinite plane, their spacing in the r direction is found to vary inversely with r. Since the gradient of the potential in any practical problem approaches zero as r increases, one intuitively seeks this type of grid (where the spacing approaches infinity as $r \to \infty$) in order to obtain uniform discretization error over the whole plane. The grid points should be spaced most closely near the region of interest where the gradient is highest. Thus, the error is expected to be low, even near the exterior interface.

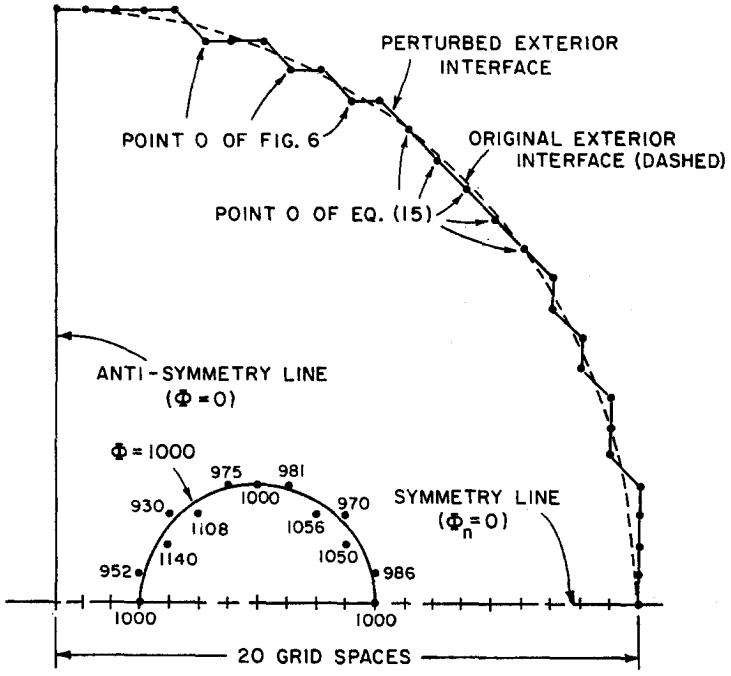

FIG. 8. Front disk of the modified exterior problem with its grid-point representation.

The accuracy of the exterior approximation is increased by an increase in a/h, the ratio of the radius of the circle of inversion to the distance between grid points. The error due to the grid point representation of the exterior interface can be controlled independently of the error due to the grid point representation of the

boundaries in the region of interest, since the latter depends only upon h. The constants selected for the problem are as follows: the grid spacing $h = 1$ unit; the radius of the exterior interface $a = 20$ units; $\epsilon = 1$; the charge density $\sigma(x, y) = 0$ everywhere (except of course on the fixed potential boundary).

The fixed potential boundary ($\Phi = 1000$) is represented by fixing the potential at nearby grid points (small dots in Fig. 8) to the correct analytical solution. At several grid points on the perturbed exterior interface, the configuration is as in Fig. 6 (compare with Fig. 8). Therefore, the difference equation used to determine the potential at these points is Eq. (14), with $Q_O = 0$. By noting the relationship between Fig. 6 and Eq. (14), it becomes clear how to write the difference equations for other points on the interface by inspection of their neighboring grid-point configurations.[5] For example, the potentials at the grid points on the 45° segment of the interface (Fig. 8) are determined by

$$4\Phi_O = \Phi_S + \Phi_{SR} + \Phi_W + \Phi_{WR} + \frac{Q_O}{\epsilon}, \tag{15}$$

where $Q_O = 0$ in this case. The finite-difference equations associated with the other grid points in the problem are five-point formulas obtained by standard techniques [6]–[8].

Solution of the set of difference equations by the successive overrelaxation method [7] required 40 seconds of computation on the Burroughs B 5500 computer. The overrelaxation factor used was that which is optimum for the square containing the same total number of grid points. The magnitude of the error in the solution, as compared with the analytical solution, was less than 0.3% of the maximum potential ($\Phi = 1000$) over the whole region of interest. The error at grid points on the perturbed interface was as high as 1.1% due to the local effects of the perturbation. However, since these perturbations alternate to either side of the original circular interface, the local errors alternate in sign; thus, their effects cancel, yielding essentially uniform error ($\leqslant 0.3\%$) over the region of interest.

This sample problem was also solved by the following method. The region of interest was enclosed by an equipotential circle ($\Phi = 0$) in order to make the problem finite. The grid-point representation used the same grid in the region of interest and the same total number of grid points (approximately the same computation time) as the above example. The error by this method reached as high as 20% of the maximum potential over the same region of interest, emphasizing the remarkable accuracy of the method described herein [6].

[5] Because of the close relationship between the difference equation associated with a point and the configuration of the neighboring grid points, the computer can be programmed to determine automatically, from the radius a alone, the difference equations which represent the exterior interface.

7. Finite-Difference Representation in r–z Coordinates

For problems in x–y coordinates, the exterior problem has been represented as a pair of two-dimensional disks, coupled at their edges; appropriate difference equations have been derived by approximating Eq. (10). The same results would have been obtained if the exterior problem had been represented as a pair of disks of finite thickness, coupled at their cylindrical edges. Then the difference equations would have been obtained by approximating Eq. (9). Because the potential does not vary with the z dimension, the thickness of the disks would have canceled out of the difference equations. Since problems in r–z coordinates are essentially three-dimensional (with axial symmetry), appropriate finite-difference approximations are derived most easily via such a three-dimensional approach.

Let the half-disks of Fig. 4 be an r–z view of a pair of wedges of "thickness" $\Delta\theta(0 < \Delta\theta \leqslant 2\pi)$. Recall that the potential Φ does not vary with θ. These wedges are connected at the exterior interface ($\rho = a$), on which is placed the charge distribution $-(\epsilon/a)\,\Phi(a, \theta, \phi)$ in order to match the boundary conditions. (Sections 3 and 4).

The wedges are perturbed at their interface in order to fit a square r–z grid of spacing h (see Fig. 9). Each wedge is represented by an identical network of grid points. Figure 9 shows the configuration of the front wedge about a point on the interface. (Viewed in the r–z half-plane, this configuration is identical with the front disk of the x–y case in Fig. 6). The point O represents both the polygonal box of

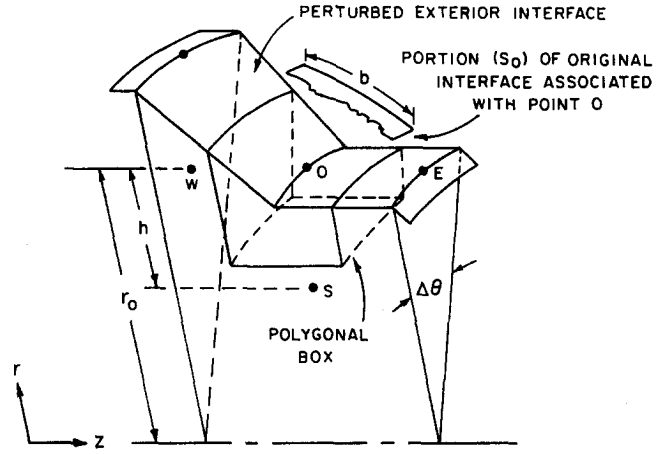

Fig. 9. Typical configuration of the front wedge about a point on the perturbed exterior interface. An identical rear wedge is distinguished by different notation for the grid points (*SR*, *WR*, etc.).

Fig. 9, which extends halfway to the neighboring grid points, and a similar box contained in the rear wedge. That portion of the perturbed interface which is associated with the point O is contained within this double polygonal box.

The difference equation which determines the potential at the point O is an algebraic approximation to Eq. (9) on the double polygonal box associated with that point. Derivatives are estimated by potential differences, and are approximately constant over each surface of the polygonal box. That portion of the flux [or the integral in Eq. (9)] which crosses the south surface S_S of the box on the front wedge is approximated by

$$\begin{aligned} -\int_{S_S} \epsilon \Phi_n \, dS &\approx -\epsilon \left(\frac{\Phi_S - \Phi_O}{h}\right) \int_{S_S} dS \\ &= -\epsilon \left(\frac{\Phi_S - \Phi_O}{h}\right)\left(r_O - \frac{h}{2}\right) \Delta\theta h \\ &= -\epsilon \left(r_O - \frac{h}{2}\right) \Delta\theta(\Phi_S - \Phi_O), \end{aligned} \tag{16}$$

where Φ_S and Φ_O are the potentials at points S and O, respectively, and $(r_O - \frac{1}{2}h)$ is the average radius of S_S. Adding together the flux crossing all external surfaces of the double polygonal box yields the following approximation to Eq. (9):

$$\begin{aligned} -\epsilon(r_O - \tfrac{1}{2}h)\,\Delta\theta(\Phi_S - \Phi_O) - \epsilon(r_O - \tfrac{1}{2}h)\,\Delta\theta(\Phi_{SR} - \Phi_O) \\ -\epsilon(r_O)\,\Delta\theta(\Phi_W - \Phi_O) - \epsilon(r_O)\,\Delta\theta(\Phi_{WR} - \Phi_O) \\ - \epsilon(r_O - \tfrac{1}{4}h)\,\Delta\theta(\Phi_E - \Phi_O) = Q_I \end{aligned} \tag{17}$$

Because of axial symmetry, no flux flows in the θ direction; therefore, no terms corresponding to the r–z faces of the polygonal box appear in Eq. (17).

Assume, for simplicity, that the charge density $\sigma(r, \theta, z)$ is zero in the neighborhood of the interface. Then the charge Q_I contained in the double polygonal box is merely that which was added to the interface in order to match the boundary conditions. The charge density on the original exterior interface is $-(\epsilon/a)\,\Phi(a,\theta,\phi)$. Therefore, the total charge on that portion S_O of the original interface which is associated with the point O is

$$Q_I = -\frac{\epsilon}{a}\int_{S_O} \Phi(a, \theta, \phi)\, r \, d\theta \, d\phi \tag{18}$$

Since $\Phi(a, \theta, \phi) \approx \Phi_O$ over the surface S_O,

$$\begin{aligned} Q_I &\approx -\frac{\epsilon}{a}\Phi_O \int_{S_O} r \, d\theta \, d\phi \\ &\approx -\frac{\epsilon}{a}\Phi_O r_O \, \Delta\theta \, b, \end{aligned} \tag{19}$$

where b is the length of the projection of S_O on the r–z half plane (see Fig. 9). Combining Eqs. (17) and (19), canceling $-\epsilon r_O \Delta\theta$, and rearranging yields

$$\left(1 - \frac{1}{2R_O}\right)(\Phi_S - \Phi_O) + \left(1 - \frac{1}{2R_O}\right)(\Phi_{SR} - \Phi_O) + (\Phi_W - \Phi_O) + (\Phi_{WR} - \Phi_O) + \left(1 - \frac{1}{4R_O}\right)(\Phi_E - \Phi_O) = \frac{b}{a}\Phi_O , \tag{20}$$

where $R_O = r_O/h$, the radius of the point O measured in grid spaces. Note that a and b can also be measured in grid spaces, since their units cancel. Putting this approximation to Poisson's equation for the neighborhood of the point O of Fig. 9 in the form

$$\left(5 - \frac{5}{4R_O} + \frac{b}{a}\right)\Phi_O = \left(1 - \frac{1}{2R_O}\right)\Phi_S + \left(1 - \frac{1}{2R_O}\right)\Phi_{SR} + \Phi_W + \Phi_{WR} + \left(1 - \frac{1}{4R_O}\right)\Phi_E \tag{21}$$

allows comparison to the two-dimensional case, Eq. (14). This comparison demonstrates both the effect of the charge on the interface (i.e., the term b/a) and the effect of r–z coordinates in general.[6]

8. Example with Axial Symmetry

The potential distribution about a pair of point charges is well known [5]; the equipotentials are spheroidal as shown in Fig. 10. A pair of these equipotentials (in this case $\Phi = \pm 1000$) can be considered as a pair of charged conductors which determine exactly the same exterior potential distribution. Because of symmetry in the configuration, the northeast quadrant of the problem is sufficient to define this potential distribution.

Figure 11 shows the grid-point representation of the northeast quadrant (r–z coordinates). The constants selected for the problem are: the grid spacing $h = 1$ unit; the radius of the exterior interface $a = 20$ units; $\epsilon = 1$; $\sigma(r, z) = 0$ (except on the fixed potential boundary and the exterior interface). The fixed potential boundary ($\Phi = 1000$) is treated in the same manner as in the two-dimensional example.

At several points on the perturbed exterior interface the configuration is as in Fig. 9; the corresponding difference equation is Eq. (21). The difference equations

[6] Since b/a is positive, Eq. (21) preserves diagonal dominance.

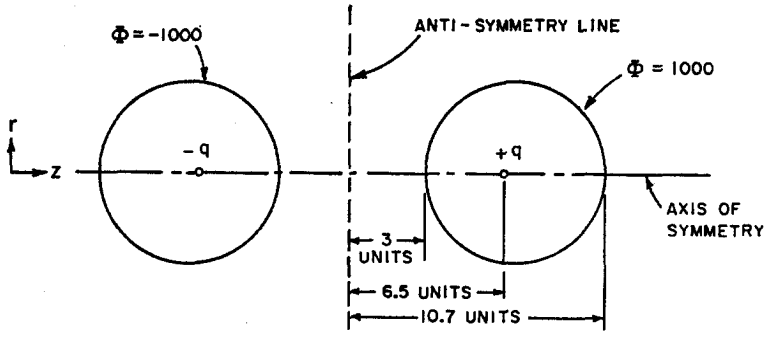

FIG. 10. Spheroidal equipotentials about a pair of opposite point charges. The potential satisfies $\nabla^2\Phi = 0$.

corresponding to other points on the exterior interface can be derived as in the previous section. On the other hand, after recognizing the relationship between the configuration of Fig. 9 and the weights on the potentials at the grid points [Eq. (20)], it is clear how to write directly the difference equation corresponding to a point by inspection of its neighboring grid-point configuration. For example, the difference equation corresponding to any point on the 45° segment of the perturbed interface (Fig. 11) is

$$\left(1 - \frac{1}{2R_O}\right)(\Phi_S - \Phi_O) + \left(1 - \frac{1}{2R_O}\right)(\Phi_{SR} - \Phi_O)$$

$$+ (\Phi_W - \Phi_O) + (\Phi_{WR} - \Phi_O) = \frac{b}{a}\Phi_O . \tag{22}$$

Each difference equation which represents a point on the exterior interface requires knowledge of b, the length of the segment of the original interface associated with that point. For this problem it is assumed that each grid point represents an equal portion of the interface in each quadrant, $b = 2\pi a/4(28)$ or $b/a = 0.5607$. The finite-difference equations associated with the other grid points in the problem are five-point formulas obtained by standard techniques [6], [9].

Solution of the set of difference equations by the successive over-relaxation method required 45 seconds of computation on the Burroughs B 5500. The error was essentially uniform over the region of interest, with a maximum magnitude of 0.3% of the maximum potential ($\Phi = 1000$). As in the two-dimensional example, local effects of the perturbation of the exterior interface resulted in an error as high as 0.6% at points actually on the interface. Although the term b/a, which represents the effect of the charge distribution on the exterior interface, only

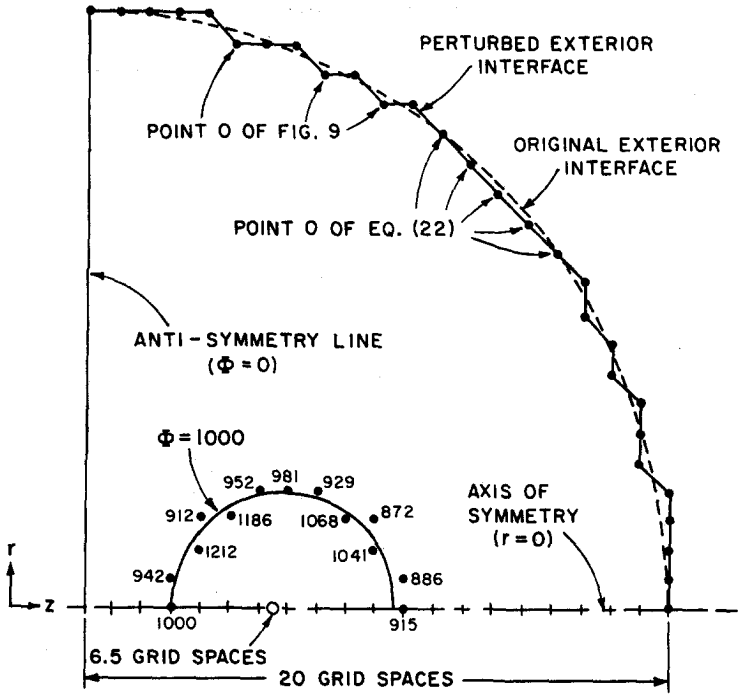

FIG. 11. Grid-point representation of northeast quadrant of Fig. 10.

slightly affects the total coefficient on the potential (Φ_o) at the point, it cannot be ignored; the above example was repeated while neglecting this charge on the interface, resulting in an error as high as 6% in the region of interest.

9. SUMMARY

The mapping concept of Boothroyd *et al.* [3] has been modified and used to convert the axially-symmetric exterior problem to an equivalent interior problem with the same region of interest. This new problem is suitable for computer solution by standard finite difference methods.

That approximation to the exterior interface which is proposed herein provides accuracy in the region of interest which is adequate for most engineering problems. Yet, the approximation is simple enough to allow the computer to handle the "exterior part" of the problem with no user intervention. In addition, those properties of the difference equations which guarantee convergence of the standard relaxation methods of solution are preserved by this approach.

ACKNOWLEDGMENT

This work was supported in part by the Westinghouse Research Laboratories. The Computer Science Center of Stanford University provided time on the B 5500 computer.

REFERENCES

1. J. E. MATHESON AND D. G. LUENBERGER, Magnetic structure design aided by a digital computer. Research Report 64-1D3-295-R1 (November 1964). Westinghouse Research Laboratories, Pittsburgh, Pennsylvania.
2. W. D. RYAN, A resistance network with quasi-infinite boundaries. *Trans. IEEE Circuit Theory* **CT-10**, 385–391 (1963).
3. A. R. BOOTHROYD, E. C. CHERRY AND R. MAKAR, An electrolytic tank for the measurement of steady-state response, transient response and allied properties of networks. *Proc. IEE* **96**, 163–177 (1949).
4. O. D. KELLOGG, "Foundations of Potential Theory." Ungar, New York, 1929.
5. E. WEBER, "Electromagnetic Fields," Vol. I. Wiley, New York, 1950.
6. C. N. DORNY, Boundary approximations in the computer solution of Poisson's equation. Report CCS-3 (August 1965). Institute in Engineering Economic Systems, Stanford University, Stanford, California.
7. G. E. FORSYTHE AND W. R. WASOW, "Finite-Difference Methods for Partial Differential Equations." Wiley, New York, 1960.
8. R. S. VARGA, "Matrix Iterative Analysis." Prentice-Hall, Englewood Cliffs, New Jersey, 1962.
9. D. GREENSPAN, Approximate solution of axially symmetric problems. *Commun. ACM* **7**, 373–377 (1964).